Structure and Dynamics of Biological Systems: Integration of Neutron Scattering with Computer Simulation

J.C. Smith, M. Krishnan, L. Petridis, N. Smolin (Oak Ridge National Laboratory)

The combination of molecular dynamics simulation and neutron scattering techniques has emerged as a highly synergistic approach to elucidate the atomistic details of the structure, dynamics and functions of biological systems. Simulation models can be tested by calculating neutron scattering structure factors and comparing the results directly with experiments. If the scattering profiles agree the simulations can be used to provide a detailed decomposition and interpretation of the experiments, and if not, the models can be rationally adjusted. Comparison with neutron experiment can be made at the level of the scattering functions or, less directly, of structural and dynamical quantities derived from them. Here, we examine the combination of simulation and experiment in the interpretation of SANS and inelastic scattering experiments on the structure and dynamics of proteins and other biopolymers.

Introduction

The characterization of the structure and internal dynamics of biomolecules such as proteins is essential to understanding the mechanisms of their biological functions. A wide range of experimental techniques has been deployed to elucidate the nature of the functional dynamics of these biomolecules (1). Among these, the combination of molecular dynamics simulation and neutron scattering techniques has emerged as a highly synergistic approach to elucidate the dynamics of biological systems. Neutron scattering can be used to test molecular simulation models by direct comparison. This can be done in two ways. The first involves directly comparing experimental and calculated scattering intensities. Secondly, one can indirectly compare experiment and simulation by examining "derived" quantities, such as the radius of gyration and the fractal dimensions of the biomolecules. However, obtaining these derived quantities from experiments and simulation requires approximations and model-dependent data interpretation.

Having made the comparison with experiments, computer simulation can be then used in the theoretical interpretation of experimental data. For example, in small-angle neutron scattering (SANS) heterogeneous, multi-component biological systems produce complex neutron scattering patterns that can be difficult to interpret, especially when the scattering length densities of the different components are similar. This problem is circumvented experimentally by the use of contrast variation techniques that make it possible to separate scattering that results from the different components through the controlled replacement of hydrogen with deuterium. The complex task of identifying scattering contributions from the various components is simplified with the use of computer simulation. Once MD simulation has been performed, it is straightforward to compute scattering intensities of the whole system or of the individual components. In other words, MD simulation can be considered as a "virtual contrast variation" technique.

This chapter provides an overview of combined applications of neutron scattering experiments and computer simulations to understand molecular motions of proteins and biopolymers. Specifically this chapter covers developments in the applications of dynamic neutron scattering to understand the protein glass transition and role of solvent interactions in controlling protein dynamics, and SANS to develop atomic resolution models of large biomolecular complexes.

Neutron Scattering Functions and Atomic Fluctuations

This chapter begins with a brief introduction to some basic equations relating neutron scattering to atomistic dynamics that are relevant to computer simulation.

In biological neutron scattering experiments, neutron beams of suitable wavelengths and energies are directed at a biological sample. When neutrons pass through the sample, they are scattered by atomic nuclei of the sample, which results in changes in the energy and momentum of the incident neutrons. By measuring these changes, information about the structure and internal dynamics of atoms/molecules that make up the sample can be inferred (2).

In neutron scattering experiments, one measures the number of neutrons scattered within a solid angle between Ω and $\Omega+d\Omega$ with a change in energy $\hbar\omega$ and momentum $\hbar\mathbf{Q}$. This number is proportional to the double-differential cross-section $\delta^2\sigma/\delta\Omega\delta\omega$, which in turn is proportional to the dynamic structure factor, $S(\mathbf{Q},\omega)$, (2):

$$\frac{\partial^2\sigma}{\partial\Omega\partial\omega} \quad \alpha \quad S(Q,\omega), \tag{1}$$

The dynamic structure factor can be written in terms of the van Hove function, $G(\mathbf{r},t)$, which characterizes the space-time correlation of individual atoms as well as between pairs of atoms, as shown in Fig. 1. It is evident from Fig. 1 that Fourier transformation of physical

quantities determining atomic dynamics in the "Molecular Dynamics Space" leads to information determined in "Neutron Scattering Space" and vice versa.

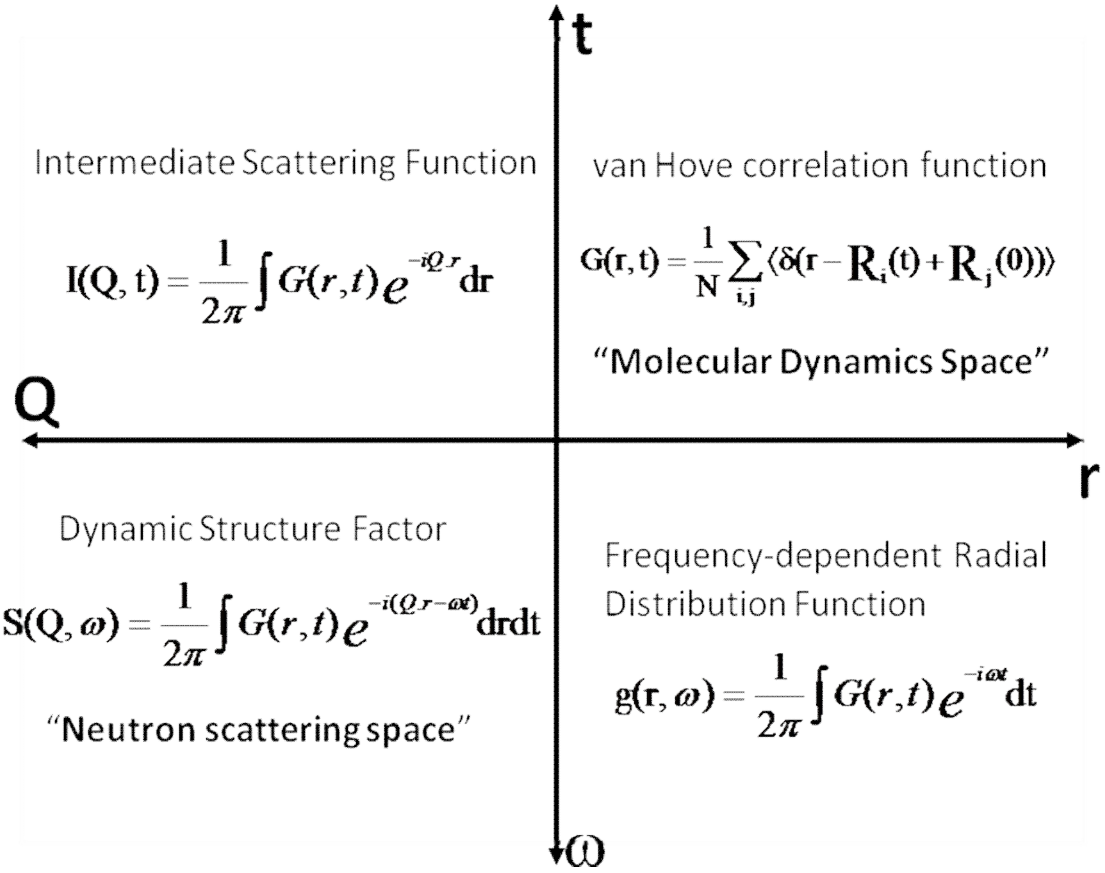

Figure 1: Schematic representation of the relationship between neutron scattering functions (determined from experiments) and the space-time correlation function (calculated using MD simulations) is shown here. Here, $\mathbf{R}_i(t)$ denotes the atomic coordinates of i^{th} atom at time t.

Small Angle Neutron Scattering (SANS)

In Small Angle Neutron Scattering (SANS) experiments one measures the flux of neutrons of wavelength λ scattered into an angle θ. The scattering intensity $I(Q)$ is a function of the scattering vector

$$I(Q) \propto P(Q) \cdot S(Q), \quad Q = \frac{2\pi}{\lambda} \sin\left(\frac{\theta}{2}\right), \tag{2}$$

where $P(Q)$ is the particle form factor and S(Q) the particle structure factor. The proportionality sign in Equation 2 accounts for instrument-specific factors. SANS intensity profiles are obtained

by examining scattering bodies, ensembles of particles that scatter in identical way, for example a scattering body may be a solid sphere that is made of tightly packed atoms. The form factor $P(Q)$ takes into account interference effects between scattering by different atoms of the same scattering body and is give by:

$$P(Q) = \frac{1}{N_p} \int n(r) \exp[i\mathbf{Q} \cdot \mathbf{r}] \, d\mathbf{r}, \tag{3}$$

where N_p is the total number of atoms in the scattering body and the scattered density $n(r) = \sum_{i=1}^{N_p} \delta(\mathbf{r} - \mathbf{r}_i)$ ($\boldsymbol{r_i}$ is the coordinate of the i^{th} atom). $P(Q)$ is determined by the overall shape of the scattering body.

In this work we will focus on the coherent scattering structure factor $S(Q)$ that is given by:

$$S(Q) = 4\pi\rho \int r^2 [g(r) - 1] \frac{\sin(Qr)}{Qr} \, dr, \tag{4}$$

where $g(r)$ is the pair-correlation function and ρ is the density of the scattering particles. The structure factor describes how *I(Q)* is modulated by interference effects between radiation scattered by different scattering bodies and can be used to gain information about the relative positions of these scattering bodies.

The combination of simulations and SANS is commonly employed to construct structural models of biological systems (3). One application is rigid body modeling, where a high-resolution structure is fit to a model that can describe correctly the experimental SANS data. Rigid body modeling can be improved by allowing configurational flexibility to the structures via the use of coarse-grained molecular dynamics simulation (4). In the absence of high resolution structures macromolecular shapes can be reconstructed *ab initio*, by placing dummy "solvent" and "sample" atoms and employing Monte-Carlo-based switching between solvent and

sample atoms (5-7). Here we focus on a third application, where SANS profiles are directly calculated from MD trajectories (8-11).

Applications of Neutron Scattering and MD simulations to Biomolecular Dynamics

Protein Glass Transition:

Neutron scattering has been a major technique in protein glass transition research. Following the first neutron scattering experiment reporting glass transition behavior on hydrated myoglobin powders (12, 13), it was demonstrated that the same transition is present in protein MD simulation (14). Subsequently, a number of neutron scattering and other experimental and computer simulation studies on various biological systems have revealed that many proteins exhibit this temperature-dependent dynamical transition around 180-220K (12, 13, 15-31). Below this transition, the dynamics is similar to that of a glassy material, while at temperatures above ~220K, protein atoms exhibit liquid-like dynamics (32).

The evidence so far points to the glass transition being a general phenomena among proteins. Furthermore, in some proteins correlations have been observed between the onset of protein function, such as ligand binding or proton pumping and the onset of the transition i.e., it has been suggested that these proteins function only when the temperature is above the dynamical transition, although enzyme function below the transition has been demonstrated (23). The 180-220K transition is sensitive to changes in solvent conditions. For example, proteins immersed in viscous solvents, such as trehalose, exhibit no transition (33).

The above observations led to the following questions concerning the microscopic dynamical details of the protein glass transition: (a) Is the dynamical transition in a solvated

protein controlled by the solvent or does the intrinsic anharmonicity of protein dynamics also play a role? (b) Do proteins exhibit intrinsic anharmonic dynamics below the glass transition temperature?

The change in gradient of mean-square displacement (MSD) versus T is consistent with the dynamics of a protein changing from harmonic to anharmonic across the transition. However, neutron scattering experiments and molecular dynamics simulations have shown signatures of anharmonic dynamics well below the ~220K dynamical transition (24, 29-31). The dynamic processes associated with this low-temperature anharmonicity, and how these motions may be related to global dynamical changes at the dynamical transition, have yet to be fully understood.

A recent neutron scattering study on hen egg-white lysozyme showed the existence of a low-temperature onset of anharmonicity at around 100K, the origin of which was suggested to be methyl group rotation (30, 31). Indeed, in neutron scattering experiments, the main contribution to the scattered protein intensity arises from the nonexchangeable hydrogen atoms, and significant fraction of nonexchangeable hydrogens in proteins resides on CH_3 groups: 26% in lysozyme, for example. Thus, the CH_3 groups contribute significantly to the scattered intensity. Also, it has been suggested that a dominant contribution of the relaxation observed in dry myoglobin neutron scattering is due to methyl dynamics (19). ^{1}H NMR relaxation studies have also investigated the reorientational dynamics of C-H bond vectors of methyl groups, and ^{1}H NMR experiments on dry lysozyme have shown that 70% of the total proton relaxation is due to methyl dynamics (34).

The MSD of atoms of hydrated myoglobin as a function of temperature calculated from recent MD simulations is shown in Figure 2 (35). The MSD increases linearly at low temperatures then exhibits two slope changes: one at ~150 K and the other at ~220 K. The change at ~220 K is the solvent-driven dynamical transition as observed in many biological

systems. At 150K, rotational excitations of methyl groups were observed in the MD and these jump-like motions of methyl protons will lead to quasi-elastic neutron scattering of the type that has been observed experimentally at ~150K in proteins (30, 31, 35). In lysozyme, the low-temperature anharmonicity was observed at 100 K and was attributed to the onset of methyl dynamics. It was also demonstrated that the anharmonic dynamics observed at ~100 K is independent of hydration level, while the dynamical transition at ~200-220K is observed only at hydration levels greater than 0.2 g water/g protein (36). Thus, recent neutron scattering experiments and MD simulations have demonstrated the non-negligible role of intrinsic anharmonicity of protein dynamics in protein glass transition.

a)

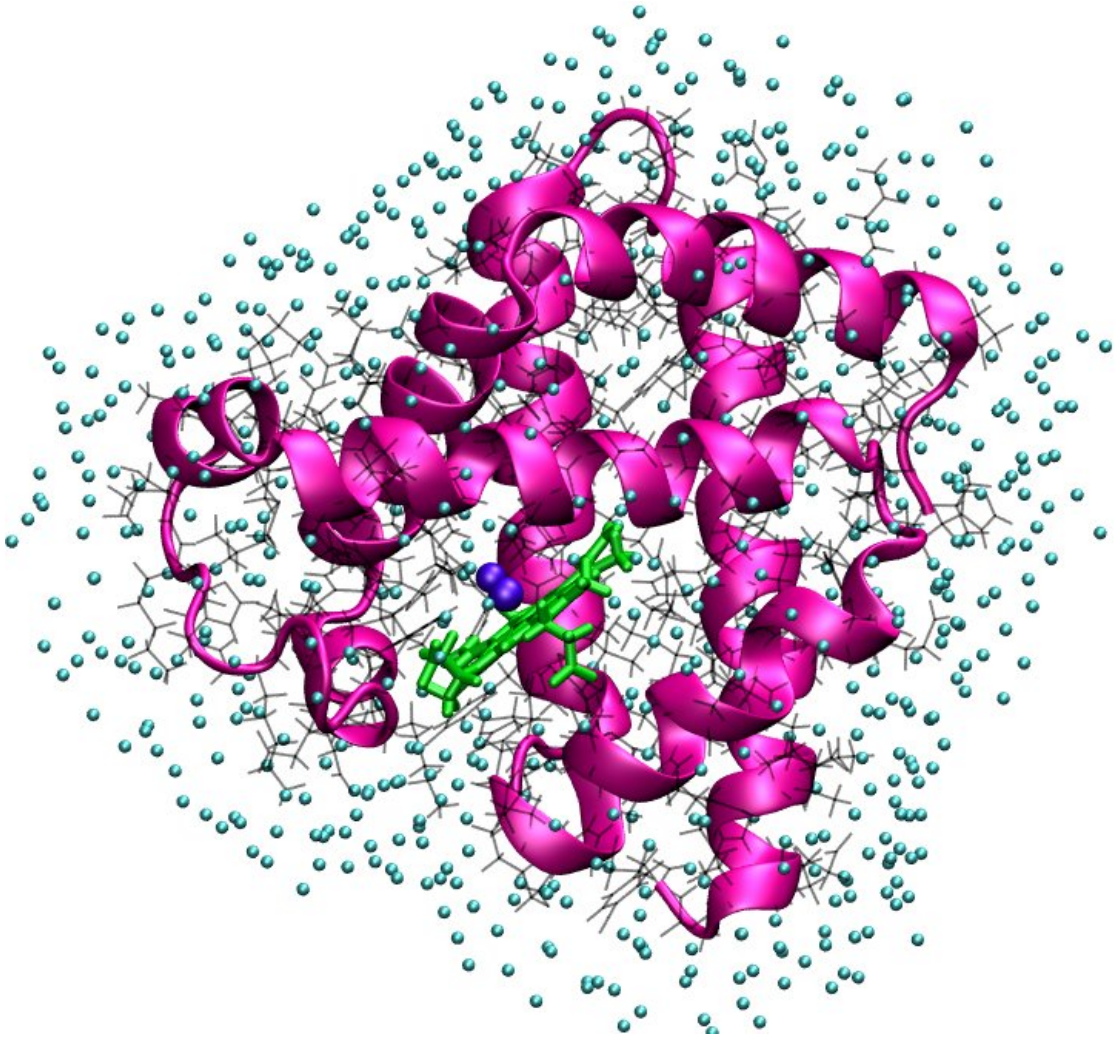

b)

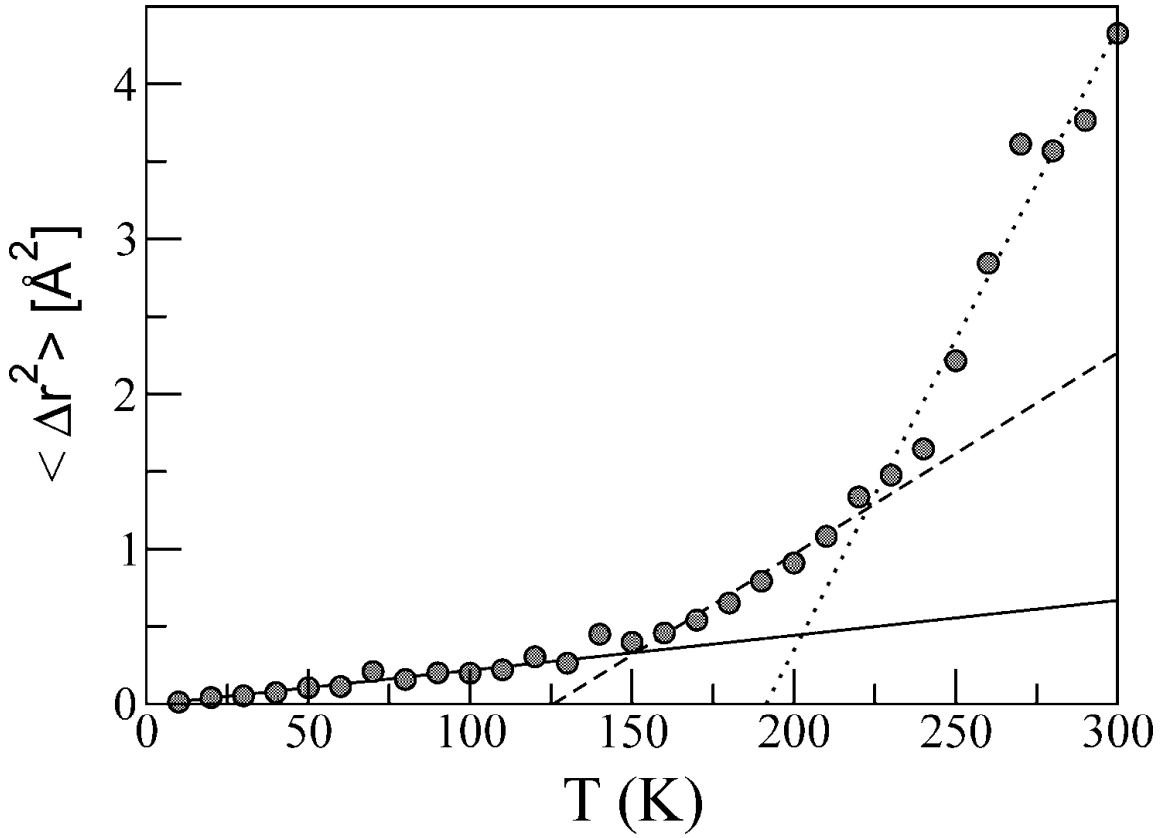

Figure 2: (a) Hydrated myoglobin is shown (purple: new cartoon representation; black: lines representation) together with water molecules (cyan: water oxygen atoms), heme (green) and carbon monoxide (violet). Water molecules that are present in the first two hydration shells around the protein are shown. (b) Time-averaged mean square displacement of myoglobin as a function of temperature from MD. The straight lines are fits to the data for different temperature ranges (solid line, 0 to 150 K; dashed line, 150 to 220 K; dotted line, above 220 K) and are shown as a guide to the eye. (Reproduced with permission from (35). Copyright 2008 Am. Chem. Soc.)

Protein-Solvent Dynamical Coupling

Water plays a crucial role in determining the structures, dynamics and function of biomolecules. Water molecules in the hydration layer of biomolecules (biological water) are important not only for the thermodynamic stability of proteins, but also play a central role in several biomolecular functionalities, such as interaction, catalysis, recognition, etc. H/D contrast technique is often used to decompose the dynamics of proteins from that of solvent. In H/D contrast technique, water and protein motions can be probed separately by measuring deuterated protein samples hydrated in H_2O and natural-abundance proteins in D_2O, respectively (37-39). A

number of experiments and simulations have indicated that when a protein is solvated the dynamical transition is strongly coupled to the solvent (20, 33, 40-44).

To determine the driving force behind the protein glass transition, a set of molecular dynamics simulations of myoglobin surrounded by a shell of water were performed using a dual heat bath method, in which the protein and solvent are held at different temperatures, at various temperatures of the components (27). The results show that the protein transition is driven by a dynamical transition in the hydration water that induces increased fluctuations primarily in sidechains in the external regions of the protein. The water transition involves activation of translational diffusion and occurs even in simulations where the protein atoms are held fixed (27, 45).

Fig. 3a presents the protein fluctuations calculated from a control set of simulations (in which in each simulation the protein and solvent are at the same temperature), together with those obtained by fixing the temperature of one component at a temperature below the dynamical transition while varying the temperature of the other. In the control set, the experimentally-known dynamical transition is reproduced, with nonlinearity starting at 220 K. Fixing the solvent temperature at 80 K or 180 K suppresses the dynamical transition, the protein MSD increasing linearly with temperature up to 300 K. Therefore, low temperature solvent cages the protein dynamics.

Fig. 3a also shows that holding the protein temperature constant at 80 K or 180 K and varying the solvent temperature also abolishes the dynamical transition behavior in the protein. In summary, then, Fig. 3a demonstrates that holding either component at a low temperature suppresses the protein dynamical transition.

Fig. 3, b and c, shows the effect of holding one component above the transition temperature while varying the temperature of the other. Holding the solvent temperature at 300 K (Fig. 3 b) leads to increased protein fluctuations at most temperatures relative to the other simulation sets. However, there is again no clear deviation from linearity, i.e., no dynamical

transition behavior. In contrast, fixing the protein at 300 K and varying the solvent temperature (Fig. 1 c) recovers dynamical transition behavior in the protein, incipient at ~200 K, a slightly lower temperature than in the control set.

When fixing the solvent at 300 K, only effects due to changes with temperature in the sampled region of the protein energy landscape appear. The absence of a dynamical transition indicates, then, that these changes do not control the transition. However, when the protein is held at 300 K, variations with temperature in the sampled solvent landscape trigger the protein transition.

Figure 4 shows the side-chain fluctuations in the control simulations as a function of distance from the protein center of mass. The dynamical transition is seen to be most pronounced in the outer parts of the protein, i.e., those close to the solvent shell—above the transition the outer shells exhibit both stronger fluctuations and a larger change in gradient (inset, Fig. 4) than the inner atoms. The solvent transition drives dynamical transition behavior primarily in the side-chain atoms of the external protein regions, i.e., those closest to the solvent.

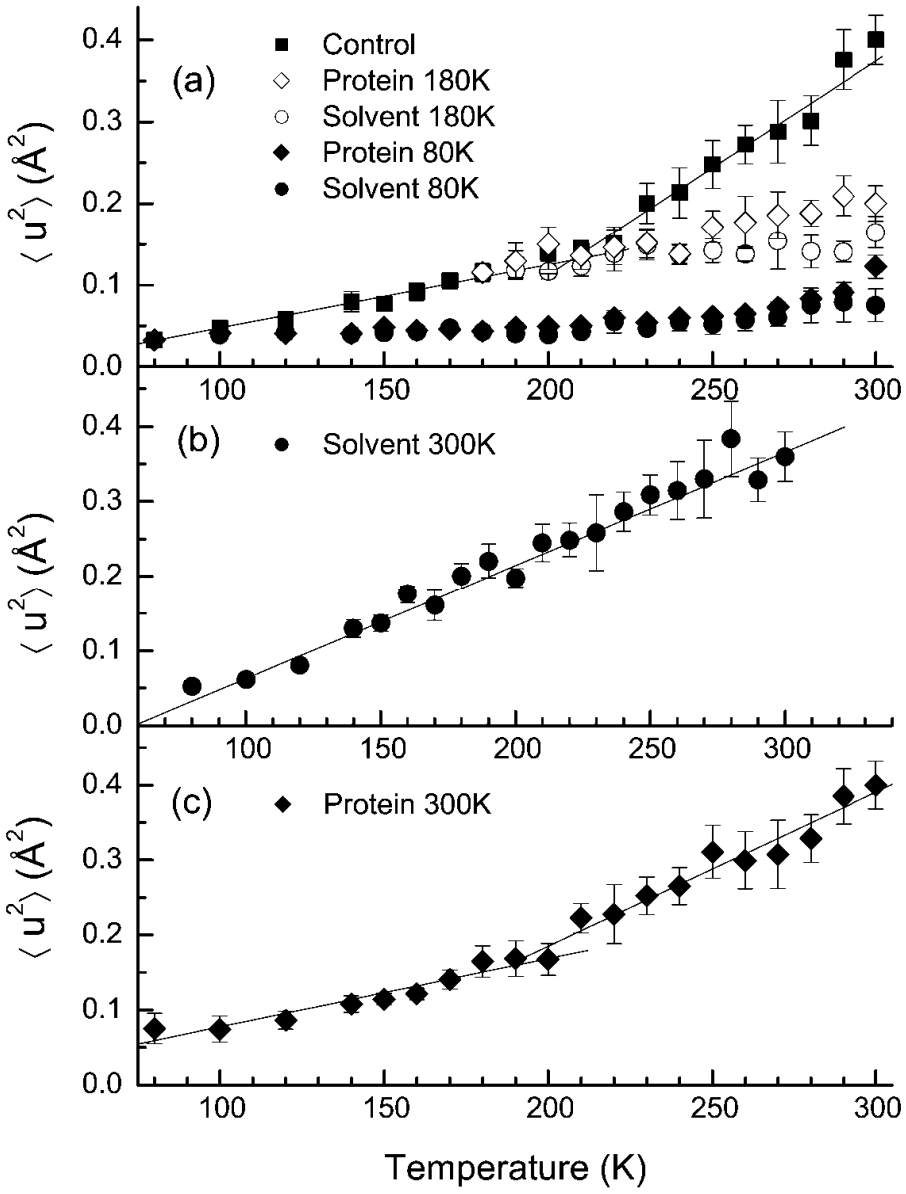

Figure 3: Mean-square fluctuations of the protein nonhydrogen atoms for different sets of simulations. (a) ■, control set with protein and solvent at same temperature; ♦, protein held at 80 K; ●, solvent held at 80 K; ◊, protein held at 180 K; ○, solvent held at 180 K. (b) Solvent held 300 K. (c) Protein held at 300 K. Figure reproduced from (27).

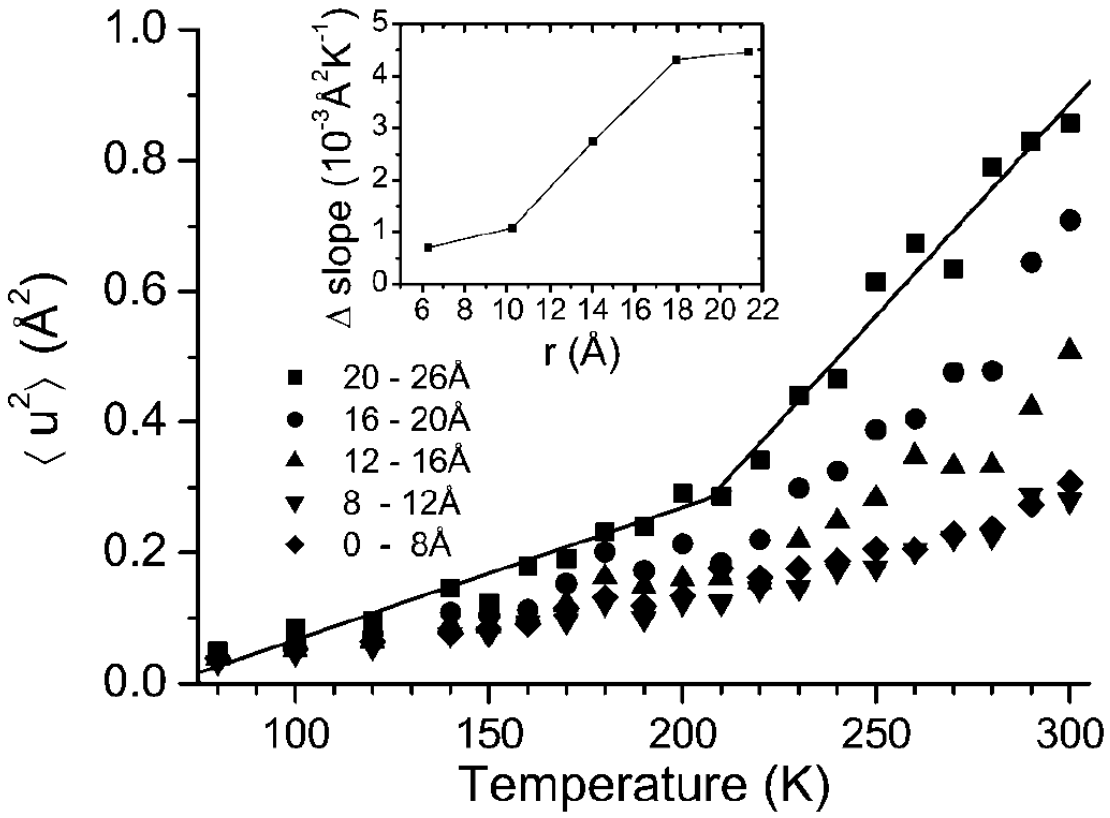

Figure 4: Mean-square fluctuations of the protein side-chain heavy atoms for five different shells, each 4 Å thick (except for the inner shell (8 Å) and outer shell (6 Å)). The inset shows the difference in slopes of lines fitted below and above 220 K as a function of distance from the protein center of mass. Linear fits to the data above and below 220 K are also shown for the outermost shell. Figure reproduced from (27).

It is believed that hydration is crucial for enzyme catalytic function, that dry enzymes are nonfunctional (36, 46), and that, below a threshold hydration level, enzymes are inactive. Experimental work on protonic conductivity of protein powders is consistent with a two-dimensional percolation transition of hydration water at the surfaces of various proteins upon increasing of the hydration level (36). Computer simulations have shown that, upon increasing the hydration level, water molecules form a spanning hydrogen-bonded network enveloping protein (47-51). Formation of this water network may play a role in collective dynamics, as a hydrogen-bonded network of water molecules may in principle exhibit dynamics which is not present in disconnected groups.

Recently, the relationship between enzyme dynamics and activity at low hydration was examined (24, 52, 53). It was found that significant intraprotein quasielastic scattering exists even below the dynamical transition. Furthermore, measurements have demonstrated enzyme activity at hydrations as low as 3% (53).

The temperature dependence of the dynamics of mesophilic and thermophilic dihydrofolate reductase has been examined using elastic incoherent neutron scattering (54). It was demonstrated that the distribution of atomic displacement (mean square displacement) amplitudes can be derived from the elastic scattering data by assuming a (Weibull) functional form (54) that resembles distributions seen in molecular dynamics simulations. A particular advantage of using the Weibull model is that the distribution of atomic fluctuation amplitudes can be estimated. Although the Weibull model has only two adjustable parameters, the combination of a power low and an exponential function confers versatility on the distribution profile. The thermophilic enzyme has found to have a significantly broader distribution than its mesophilic counterpart. Furthermore, although the rate of increase with temperature of the atomic mean-square displacements extracted from the dynamic structure factor was found to be comparable for both enzymes, the amplitudes were found to be slightly larger for the thermophilic enzyme. Therefore, these results imply that the thermophilic enzyme is the more flexible of the two.

A physical characterization of protein-protein interactions is very important for understanding the mechanics of cell function. Recently reported all-atom lattice-dynamical calculations for a crystalline protein, ribonuclease A, showed that the sound velocities, density of states, heat capacity (C_V) and thermal diffuse scattering are all consistent with available experimental data (55). C_V was found to be proportional to $T^{-1.68}$ for $T < 35$ K, significantly deviating from a Debye solid. In the vicinity of Bragg peak, inelastic scattering of X-rays by phonons was found to originate from acoustic mode scattering. The results suggest an approach

to protein crystal physics combining all-atom lattice-dynamical calculations with experiments on next-generation neutron sources.

Furthermore, interprotein motions in low and fully hydrated carboxymyoglobin crystals were investigated using molecular dynamics simulation (56). Below ≈ 240 K, the calculated dynamic structure factor showed a peak arising from interprotein vibration. Above ≈ 240 K, the intermolecular fluctuations of the fully hydrated crystal increase drastically, whereas the low-hydration model exhibits no transition. Autocorrelation function analysis demonstrated the transition to be dominated by the activation of diffusive intermolecular motion. The potential of mean force for the interaction remains quasiharmonic. In recent work using molecular dynamics simulation it was shown that above 240 K, the intermolecular fluctuations of the fully hydrated protein crystal increase drastically, whereas a low-hydration model exhibits no transition (56).

Finally, we draw attention to work designed to derive simplified analytical models for diffusive protein dynamics. Molecular dynamics simulation of oligopeptide chains reveals configurational subdiffusion at equilibrium extending from 10^{-12} to 10^{-8} s. Trap models, involving a random walk with a distribution of waiting times, cannot account for the subdiffusion, which has found rather to arise from the fractal-like structure of the accessible configuration space (57). These conceptual approaches will hopefully be of use in analysing quasielastic scattering.

Density of Protein Hydration Shell

We now present an example of the use of experimental SANS data used to test computational models. Several studies have indicated that it is necessary to take into account hydration effects in SAS studies (9, 58, 59). MD simulation provides an interpretation of neutron solution scattering data in terms of the density of water on the surface of lysozyme (9). The simulation-derived scattering profiles are in excellent agreement with the experiment. In the

simulation, the 3-Å-thick first hydration layer was found to be 15% denser than bulk water. About two-thirds of this increase is the result of a geometric contribution that would also be present if the water was unperturbed from the bulk. The remaining third arises from modification of the water structure and dynamics.

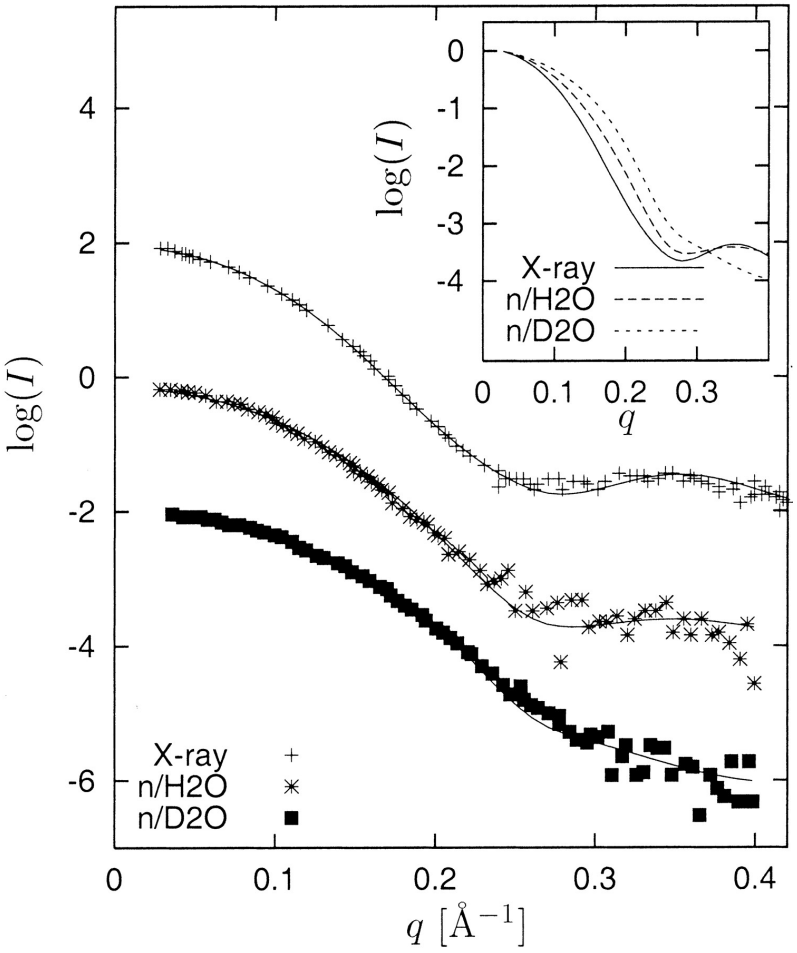

Figure 5: Comparison of MD calculated (solid lines) with experimental x-ray and neutron SAS profiles (taken from ref. (9)). In the main figure the y axis of different profiles is shifted for clarity. Inset shows calculated SAS intensities with common origin.

Structural Analysis of Lignocellulose

SANS is especially well suited for studying disordered polymers. Theoretical approaches to interpret the scattering include treating the disorder polymers as fractals (60). Fractals are self-similar objects whose structure remains invariant under magnification (61). Various biological systems are known to be fractals, such as biomembranes and antbody aggregates (62). The use of

analogy with fractals in the context of SANS originates from the experimental observation that the scattering intensity $I(Q)$ is often proportional to a negative power of the scattering vector, Q:

$$I(Q) \propto Q^{-\alpha}, \tag{5}$$

where α is the power-law exponent. This power-law behavior is typical of fractal systems and useful information about the system can be deduced from the value of the exponent α.

When discussing SANS, it is important to consider two types of fractals: mass fractals and surface fractals (61). Mass fractals are objects for which the scaling relation gives the mass, M inside a sphere of radius, R:

$$M(R) \propto R^{D_m}, \tag{6}$$

where $D_m \leq 3$ is the mass-fractal dimension. In contrast, surface fractals are better understood by considering the space filling ability of a curve or surface (63). Their properties are determined by the surface-fractal dimension, D_s that takes values $2<D_s<3$. The surface fractal dimension is best understood by imagining that the surface of a molecule is covered with a monolayer of spheres of radius r. Let $N(r)$ be the number of such spheres required to fully cover the surface of the molecule, then:

$$N(r) \propto r^{-D_s}. \tag{7}$$

The above two fractal dimensions provide examples of derived quantities that can be used to compare simulation with experiments. D_s and D_m can be obtained using two separate approaches: firstly, by analyzing the scattering intensities obtained experimentally or calculated from MD trajectories. As mentioned earlier SANS intensities often display a power-law dependence on the wave vector, see Equation (5), and the exponent α is directly related to the fractal dimension of the biomolecule. If $1<\alpha<3$, then mass-fractal scattering is observed and $\alpha = D_m$. If $3<\alpha<4$, then surface scattering is observed and now $\alpha = 6 - D_s$. The power-law exponent α can be measured directly either from the slope of lnI vs lnq, or, more accurately, using the so-called "unified approach" to analyze SANS data (64). The unified approach

describes scattering from complex systems that contain many structural levels: one level described by a Guinier and an associated power-law regime. A function is derived that models both the Guinier exponential and structurally limited power-law regimes. For more information see Ref. (64).

The second way to obtain values for the fractal dimensions of biopolymers is through analysis of the atomic-coordinate information of MD trajectories, i.e., without computing SANS spectra. Polymer theory provides a computationally straightforward way to obtain the mass-fractal dimension by linking the easily-calculated radius of gyration of a polymer with the total number of monomers N comprising the polymer:

$$R_g \propto N^{1/D_m}. \tag{8}$$

Depending on the interactions between the solvent and the solute, the theory predicts only three possible values for D_m=5/3, 2 and 3, for good-, theta- and bad solvents, respectively. To obtain the surface-fractal dimension one computes the Surface Accessible Surface Area (SASA). This is done by rolling a sphere of radius r on the surface of the molecule and then using the points visited by the center of the sphere to define a surface. The observed surface area is a function of the size of the probe radius, as using a smaller probe detects more surface details leading to a larger surface area. For a surface fractal covered with N such spheres of radius r the SASA is given by:

$$A(r) \propto N \cdot r^2 \propto r^{-D_s+2}, \tag{9}$$

the second relation obtained using Equation 7.

It is hoped that in the future the mass fractal and surface fractal approaches will be usefull in understanding lignocellulostic biomass. Lignocellulose is a complex biomaterial made of cellulose microfibrils embedded in a matrix of polysaccharides (hemicellulose and pectins) and lignin (65). Its structural analysis requires characterization techniques capable of spanning many

length scales (from angstroms to micrometers) while differentiating between the components, such as lignin, hemicellulose and cellulose. SANS is ideally suited to this task because it can probe the length scales appropriate for lignocellulose characterization, and, furthermore, neutron scattering enables contrast variation techniques that make it possible to separate scattering results for different compounds within intact lignocellulose through the controlled replacement of hydrogen with deuterium. Deuteration of lignocellulose, however, is a difficult task because of the toxic effect of D_2O on the germination, growth and development of plants (66).

Computer simulation can potentially bypass this experimental hurdle, since it can act as a "virtual contrast variation" technique. This is ccomplished by selecting a component (cellulose, lignin or hemicellulose) of the model and calculating the SANS profiles for this component alone. However this approach faces many challenges, including the construction of an accurate model and the mismatch between the length scales probed by experiments (up to micrometers) and simulation (up to hundreds of nanometers). This is where the fractal nature of biopolymers becomes useful: experiments show that these materials scatter as mass- or surface-fractals over a wide range of length-scales (wave-vector range $0.01\ Å^{-1} < Q < 0.05\ Å^{-1}$), the lower limit of which is accessible with all-atom MD simulation. One can then use the computational methods described above to evaluate the mass- and surface-fractal dimensions. We hope to be able to present results combining SANS with MD in the analysis of lignocellulose in the near future.

Conclusions

In this chapter, we have provided an overview of synergistic applications of various neutron scattering techniques and computer simulation to unravel atomistic details of many dynamical phenomena of physical and biological interest that occur on the subnanosecond time scale. The advent of next-generation neutron sources (such as the Spallation Neutron Source at Oak Ridge National Laboratory) together with advanced deuteration facilities and continuing

rapid increase in computing power will open up new vistas for further high-resolution insights into large length scale and long time-scale biomolecular structure and dynamics.

Acknowledgements

This research is funded in part by the Genomics:GTL Program, Office of Biological and Environmental Research, U. S. Department of Energy, under the BioEnergy Science Center. The BioEnergy Science Center is a U.S. Department of Energy Bioenergy Research Center supported by the Office of Biological and Environmental Research in the DOE Office of Science. The research is also funded in part by FWP ERKP704 "Dynamic Visualization of Lignocellulose Degradation by Integration of Neutron Scattering Imaging and Computer Simulation" funded by the DOE office of Bioscience and Environmental Research. Finally, JCS acknowledges funds from the DOE ORNL Laboratory Directed Research and Development funds (grant no: Systems Biology L00044).

References

1. Brooks, C. L., III; Karplus, M.; Pettitt, B. M. 1988. Proteins : A Theoretical Perspective of Dynamics, Structure, and Thermodynamics. Wiley, New York.
2. Bee, M. 1988. Quasielastic Neutron Scattering: Principles and Applications in Solid State Chemistry, Biology and Materials Science. Adam Hilger, Philadelphia.
3. Neylon, C. 2008. Small angle neutron and X-ray scattering in structural biology: recent examples from the literature. European Biophysics Journal with Biophysics Letters 37:531-541.
4. Yang, S. C., S. Park, L. Makowski, and B. Roux. 2009. A Rapid Coarse Residue-Based Computational Method for X-Ray Solution Scattering Characterization of Protein Folds and Multiple Conformational States of Large Protein Complexes. Biophysical Journal 96:4449-4463.
5. Svergun, D. I. 1999. Restoring low resolution structure of biological macromolecules from solution scattering using simulated annealing. Biophysical Journal 76:2879-2886.
6. Walther, D., F. E. Cohen, and S. Doniach. 2000. Reconstruction of low-resolution three-dimensional density maps from one-dimensional small-angle X-ray solution scattering data for biomolecules. J. Appl. Crystallogr. 33:350-363.
7. Heller, W. T., E. Abusamhadneh, N. Finley, P. R. Rosevear, and J. Trewhella. 2002. The solution structure of a cardiac troponin C-troponin I-troponin T complex shows a somewhat compact troponin c interacting with an extended troponin I-Troponin T component. Biochemistry 41:15654-15663.

8. Svergun, D., C. Barberato, and M. H. J. Koch. 1995. CRYSOL - A program to evaluate x-ray solution scattering of biological macromolecules from atomic coordinates. J. Appl. Crystallogr. 28:768-773.
9. Merzel, F., and J. C. Smith. 2002. Is the first hydration shell of lysozyme of higher density than bulk water? Proceedings of the National Academy of Sciences of the United States of America 99:5378-5383.
10. Tiede, D. M., R. T. Zhang, and S. Seifert. 2002. Protein conformations explored by difference high-angle solution x-ray scattering: Oxidation state and temperature dependent changes in cytochrome C. Biochemistry 41:6605-6614.
11. Tjioe, E., and W. T. Heller. 2007. ORNL_SAS: software for calculation of small-angle scattering intensities of proteins and protein complexes. J. Appl. Crystallogr. 40:782-785.
12. Doster, W., S. Cusack, and W. Petry. 1990. Dynamic Instability of Liquid-Like Motions in a Globular Protein Observed by Inelastic Neutron-Scattering. Physical Review Letters 65:1080-1083.
13. Doster, W., S. Cusack, and W. Petry. 1989. Dynamical Transition of Myoglobin Revealed by Inelastic Neutron-Scattering. Nature 337:754-756.
14. Smith, J., K. Kuczera, and M. Karplus. 1990. Dynamics of Myoglobin - Comparison of Simulation Results with Neutron-Scattering Spectra. Proceedings of the National Academy of Sciences of the United States of America 87:1601-1605.
15. Knapp, E. W., S. F. Fischer, and F. Parak. 1983. The Influence of Protein Dynamics on Mossbauer-Spectra. J. Chem. Phys. 78:4701-4711.
16. Knapp, E. W., S. F. Fischer, and F. Parak. 1982. Protein Dynamics from Mossbauer-Spectra - the Temperature-Dependence. Journal of Physical Chemistry 86:5042-5047.
17. Diehl, M., W. Doster, W. Petry, and H. Schober. 1997. Water-coupled low-frequency modes of myoglobin and lysozyme observed by inelastic neutron scattering. Biophysical Journal 73:2726-2732.
18. Reat, V., H. Patzelt, M. Ferrand, C. Pfister, D. Oesterhelt, and G. Zaccai. 1998. Dynamics of different functional parts of bacteriorhodopsin: H-H-2 labeling and neutron scattering. Proceedings of the National Academy of Sciences of the United States of America 95:4970-4975.
19. Doster, W., and M. Settles. 2005. Protein-water displacement distributions. Biochimica Et Biophysica Acta-Proteins and Proteomics 1749:173-186.
20. Reat, V., R. Dunn, M. Ferrand, J. L. Finney, P. M. Daniel, and J. C. Smith. 2000. Solvent dependence of dynamic transitions in protein solutions. Proceedings of the National Academy of Sciences of the United States of America 97:9961-9966.
21. Daniel, R. M., R. V. Dunn, J. L. Finney, and J. C. Smith. 2003. The role of dynamics in enzyme activity. Annual Review of Biophysics and Biomolecular Structure 32:69-92.
22. Daniel, R. M., J. L. Finney, V. Reat, R. Dunn, M. Ferrand, and J. C. Smith. 1999. Enzyme dynamics and activity: Time-scale dependence of dynamical transitions in glutamate dehydrogenase solution. Biophysical Journal 77:2184-2190.
23. Daniel, R. M., J. C. Smith, M. Ferrand, S. Hery, R. Dunn, and J. L. Finney. 1998. Enzyme activity below the dynamical transition at 220 K. Biophysical Journal 75:2504-2507.
24. Kurkal, V., R. M. Daniel, J. L. Finney, M. Tehei, R. V. Dunn, and J. C. Smith. 2005. Enzyme activity and flexibility at very low hydration. Biophysical Journal 89:1282-1287.
25. Brown, K. G., E. W. Small, Peticola.Wl, and S. C. Erfurth. 1972. Conformationally Dependent Low-Frequency Motions of Proteins by Laser Raman Spectroscopy. Proceedings of the National Academy of Sciences of the United States of America 69:1467-&.
26. Tournier, A. L., and J. C. Smith. 2003. Principal components of the protein dynamical transition. Physical Review Letters 91.

27. Tournier, A. L., J. C. Xu, and J. C. Smith. 2003. Translational hydration water dynamics drives the protein glass transition. Biophysical Journal 85:1871-1875.
28. Hayward, J. A., J. L. Finney, R. M. Daniel, and J. C. Smith. 2003. Molecular dynamics decomposition of temperature-dependent elastic neutron scattering by a protein solution. Biophysical Journal 85:679-685.
29. Hayward, J. A., and J. C. Smith. 2002. Temperature dependence of protein dynamics: Computer simulation analysis of neutron scattering properties. Biophysical Journal 82:1216-1225.
30. Roh, J. H., J. E. Curtis, S. Azzam, V. N. Novikov, I. Peral, Z. Chowdhuri, R. B. Gregory, and A. P. Sokolov. 2006. Influence of hydration on the dynamics of lysozyme. Biophysical Journal 91:2573-2588.
31. Roh, J. H., V. N. Novikov, R. B. Gregory, J. E. Curtis, Z. Chowdhuri, and A. P. Sokolov. 2005. Onsets of anharmonicity in protein dynamics. Physical Review Letters 95.
32. Kneller, G. R., and J. C. Smith. 1994. Liquid-Like Side-Chain Dynamics in Myoglobin. Journal of Molecular Biology 242:181-185.
33. Cordone, L., M. Ferrand, E. Vitrano, and G. Zaccai. 1999. Harmonic behavior of trehalose-coated carbon-monoxy-myoglobin at high temperature. Biophysical Journal 76:1043-1047.
34. Andrew, E. R., D. J. Bryant, and E. M. Cashell. 1980. Proton Magnetic-Relaxation of Proteins in the Solid-State - Molecular-Dynamics of Ribonuclease. Chemical Physics Letters 69:551-554.
35. Krishnan, M., V. Kurkal-Siebert, and J. C. Smith. 2008. Methyl group dynamics and the onset of anharmonicity in myoglobin. J. Phys. Chem. B 112:5522-5533.
36. Rupley, J. A., and G. Careri. 1991. Protein Hydration and Function. Advances in Protein Chemistry 41:37-172.
37. Wood, K., A. Frolich, A. Paciaroni, M. Moulin, M. Hartlein, G. Zaccai, D. J. Tobias, and M. Weik. 2008. Coincidence of dynamical transitions in a soluble protein and its hydration water: Direct measurements by neutron scattering and MD simulations. Journal of the American Chemical Society 130:4586-+.
38. Jasnin, M., M. Moulin, M. Haertlein, G. Zaccai, and M. Tehei. 2008. Down to atomic-scale intracellular water dynamics. EMBO Rep. 9:543-547.
39. Tehei, M., B. Franzetti, K. Wood, F. Gabel, E. Fabiani, M. Jasnin, M. Zamponi, D. Oesterhelt, G. Zaccai, M. Ginzburg, and B. Z. Ginzburg. 2007. Neutron scattering reveals extremely slow cell water in a Dead Sea organism. Proceedings of the National Academy of Sciences of the United States of America 104:766-771.
40. Fitter, J., R. E. Lechner, and N. A. Dencher. 1997. Picosecond molecular motions in bacteriorhodopsin from neutron scattering. Biophysical Journal 73:2126-2137.
41. Ferrand, M., A. J. Dianoux, W. Petry, and G. Zaccai. 1993. Thermal Motions and Function of Bacteriorhodopsin in Purple Membranes - Effects of Temperature and Hydration Studied by Neutron-Scattering. Proceedings of the National Academy of Sciences of the United States of America 90:9668-9672.
42. Paciaroni, A., S. Cinelli, and G. Onori. 2002. Effect of the environment on the protein dynamical transition: A neutron scattering study. Biophysical Journal 83:1157-1164.
43. Fitter, J. 1999. The temperature dependence of internal molecular motions in hydrated and dry alpha-amylase: The role of hydration water in the dynamical transition of proteins. Biophysical Journal 76:1034-1042.
44. Teeter, M. M., A. Yamano, B. Stec, and U. Mohanty. 2001. On the nature of a glassy state of matter in a hydrated protein: Relation to protein function. Proceedings of the National Academy of Sciences of the United States of America 98:11242-11247.
45. Tournier, A. L., J. C. Xu, and J. C. Smith. 2003. Solvent caging of internal motions in myoglobin at low temperatures. Physchemcomm 6:6-8.

46. Finney, J. L. 1996. Hydration processes in biological and macromolecular systems. Faraday Discussions 103:1-18.
47. Brovchenko, I., A. Krukau, N. Smolin, A. Oleinikova, A. Geiger, and R. Winter. 2005. Thermal breaking of spanning water networks in the hydration shell of proteins. J. Chem. Phys. 123:10.
48. Oleinikova, A., I. Brovchenko, N. Smolin, A. Krukau, A. Geiger, and R. Winter. 2005. Percolation transition of hydration water: From planar hydrophilic surfaces to proteins. Physical Review Letters 95:4.
49. Oleinikova, A., N. Smolin, and I. Brovchenko. 2006. Origin of the dynamic transition upon pressurization of crystalline proteins. J. Phys. Chem. B 110:19619-19624.
50. Oleinikova, A., N. Smolin, and I. Brovchenko. 2007. Influence of water clustering on the dynamics of hydration water at the surface of a lysozyme. Biophysical Journal 93:2986-3000.
51. Smolin, N., A. Oleinikova, I. Brovchenko, A. Geiger, and R. Winter. 2005. Properties of spanning water networks at protein surfaces. J. Phys. Chem. B 109:10995-11005.
52. Kurkal, V., R. M. Daniel, J. L. Finney, M. Tehei, R. V. Dunn, and J. C. Smith. 2005. Low frequency enzyme dynamics as a function of temperature and hydration: A neutron scattering study. Chemical Physics 317:267-273.
53. Kurkal-Siebert, V., R. M. Daniel, J. L. Finney, M. Tehei, R. V. Dunn, and J. C. Smith. 2006. Enzyme hydration, activity and flexibility: A neutron scattering approach. Biophysical Journal 89:4387-4393.
54. Meinhold, L., D. Clement, M. Tehei, R. Daniel, J. L. Finney, and J. C. Smith. 2008. Protein dynamics and stability: The distribution of atomic fluctuations in thermophilic and mesophilic dihydrofolate reductase derived using elastic incoherent neutron scattering. Biophysical Journal 94:4812-4818.
55. Meinhold, L., F. Merzel, and J. C. Smith. 2007. Lattice dynamics of a protein crystal. Physical Review Letters 99.
56. Kurkal-Siebert, V., R. Agarwal, and J. C. Smith. 2008. Hydration-dependent dynamical transition in protein: Protein interactions at approximate to 240 K. Physical Review Letters 100.
57. Neusius, T., I. Daidone, I. M. Sokolov, and J. C. Smith. 2008. Subdiffusion in peptides originates from the fractal-like structure of configuration space. Physical Review Letters 100.
58. Hubbard, S. R., K. O. Hodgson, and S. Doniach. 1988. Small-Angle X-Ray-Scattering Investigation of the Solution Structure of Troponin-C. Journal of Biological Chemistry 263:4151-4158.
59. Grossmann, J. G., Z. H. L. Abraham, E. T. Adman, M. Neu, R. R. Eady, B. E. Smith, and S. S. Hasnain. 1993. X-Ray-Scattering Using Synchrotron-Radiation Shows Nitrite Reductase from Achromobacter-Xylosoxidans to Be a Trimer in Solution. Biochemistry 32:7360-7366.
60. Schmidt, P. W. 1991. Small-Angle Scattering Studies of Disordered, Porous and Fractal Systems. Munksgaard Int Publ Ltd. 414-435.
61. Mandelbrot, B. B. 1983. The fractal geometry of nature. W.H. Freeman and Co.,, New York.
62. Dewey, T. G. 1997. Fractals in Molecular Biophysics. OUP, New York.
63. Pfeifer, P., and D. Avnir. 1983. Chemistry in Noninteger Dimensions between 2 and 3 .1. Fractal Theory of Heterogeneous Surfaces. J. Chem. Phys. 79:3558-3565.
64. Beaucage, G. 1995. Approximations leading to a unified exponential power-law approach to small-angle scattering. J. Appl. Crystallogr. 28:717-728.
65. Cosgrove, D. J. 2005. Growth of the plant cell wall. Nature Reviews Molecular Cell Biology 6:850-861.

66. Boudet, A., T. J. Humphrey, and D. D. Davies. 1975. Measurement of Protein Turnover by Density Labeling. Biochemical Journal 152:409-416.